

Supporting information

Penetration of the blood-brain barrier and anti-tumor effect of a novel PLGA-lysoGM1/DOX micelles drug delivery system

¹Ying Yin, ¹Jun Wang, ¹Meng Yang, ¹Ruolin Du, ³Giuseppe Pontrelli, ⁴Sean McGinty, ¹Guixue Wang, ¹Tieying Yin* and ^{1,2}Yazhou Wang*

¹Key Laboratory of Biorheological Science and Technology, Ministry of Education, College of Bioengineering, Chongqing University, Chongqing 400044, China

²Medical School of Chongqing University, Chongqing University, Chongqing 400044, China

³Istituto per le Applicazioni del Calcolo - CNR, Via dei Taurini 19, 00185 Roma, Italy

⁴Division of Biomedical Engineering, University of Glasgow, UK.

Corresponding authors: Yazhou Wang: Medical School of Chongqing University, Chongqing University, Chongqing 400044, China. Tel: 86 15803055646; Fax: 86 23 65102507; E-mail: yazhou_wang@cqu.edu.cn; Tieying Yin: Key Laboratory for Biorheological Science and Technology of Ministry of Education, State and Local Joint Engineering Laboratory for Vascular Implants, Bioengineering College of Chongqing University, Chongqing 400030, China. Tel: 86 13618289435; Fax: 86 23 65102507; E-mail: ilyyty28@126.com.

Methods

Optimizing preparation of PLGA-LysoGM1/DOX micelles: a method was developed and validated for preparing PLGA-lysoGM1/DOX micelles.¹ A stock solution of PLGA-lysoGM1 was dissolved in N, N-dimethylformamide(DMF). The solution was maintained at 4° C for 24 h, and

then centrifuged at 10,000×g for 15 min, and the supernatant was filtered through 0.22 μm filter. Then, the hydrochloric acid DOX solution was slowly added to PLGA-lysoGM1 micelles solution. The mixed micelles were incubated at 4° C for 24 h and dialyzed for 24 h to remove all the DMF. There are many factors affecting the preparation of micelles. In this paper, orthogonal experimental design (OED) method was used for constructing the best combination levels for different factors (Table S1). (A) DOX concentration (mg/mL), (B) PLGA-lysoGM1 concentration (mg/mL), and (C) Water phase/Organic phase (mL/mL) varied at three different levels when preparing micelles (Table S2). The drug loading efficiency and encapsulation efficiency of the nine combinations were analyzed according to the range analysis to determine the optimal combination (Table S4). However the ratio of the aqueous phase to the oil phase has the greatest influence on the entrapment efficiency and drug loading of the carrier polymer, followed by the carrier volume, and finally the dosage. Therefore, we reduced the aqueous phase to 5 mL, increased the PLGA-lysoGM1 polymer to 30 mg (Finally, the conditions for optimal preparation of micelles were DOX: 15 mg, carrier: 30 mg, aqueous phase: 5 mL), and prepared PLGA-lysoGM1/DOX micelles with a drug loading of 3.8% and an encapsulation efficiency of 61.6%.

Table S1. Factors and levels of the preparation of PLGA-lysoGM1/DOX micelles.

Factors Levels	A: DOX concentration(mg/mL)	B: PLGA-lysoGM1 concentration(mg/mL)	C: Water phase/Organic phase(mL/mL)
(1)L1	4	8	8/1
(2)L2	8	12	12/1
(3)L3	12	16	16/1

According to the orthogonal design requirements of L9 (3⁴), A: the concentration of DOX was

designed to be 4 mg/mL, 8 mg/mL, 12 mg/mL; B: the concentration of PLGA-lysoGM1 was 8 mg/mL, 12 mg/mL, 16 mg/mL, C: Water phase/ Organic phase (mL/mL) was 8/1, 12/1, 16/1, designed as follows 3 factors 3 horizontal orthogonal table S2.

Table S2. Orthogonal array of the OED method.

Combinations	A: DOX concentration(mg/mL)	B: PLGA-lysoGM1 concentration(mg/mL)	C: Water phase/Organic phase(mL/mL)
C1	(1) 4	(1) 8	(1) 8/1
C2	(2) 8	(2) 12	(2) 12/1
C3	(3) 12	(3) 16	(3) 16/1
C4	(1) 4	(2) 12	(3) 16/1
C5	(2) 8	(3) 16	(1) 8/1
C6	(3) 12	(1) 8	(2) 12/1
C7	(1) 4	(3) 16	(2) 12/1
C8	(2) 8	(1) 8	(3) 16/1
C9	(3) 12	(2) 12	(1) 8/1

Preparing 9 sets of PLGA-lysoGM1/DOX micelles according to the above orthogonal table.

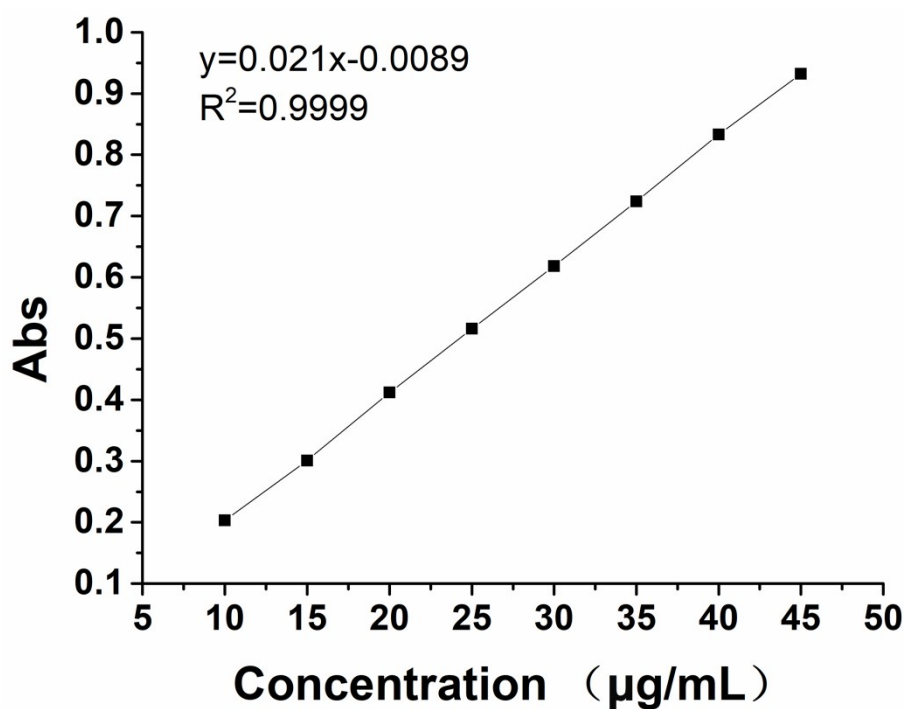


Figure S1. Standard curve of DOX in DMF solution. The regression equation is $y=0.021x-0.0089$, $R^2=0.9999$.

Therefore, the concentration of DOX has a good linear relationship with the absorbance value in the concentration range of 10-45 $\mu\text{g/mL}$.

Table S3. Loading efficiency and encapsulation efficiency.

Combinations	Loading efficiency (%)	Encapsulation efficiency (%)
1	1.540	50.012
2	2.950	56.108
3	2.074	32.389
4	0.723	36.573
5	2.543	31.531
6	3.876	54.190
7	1.173	45.116
8	1.529	36.388
9	4.706	51.064

After calculation, the drug loading and encapsulation efficiency of the 9 groups of micelle solutions are shown in Table S3. From this result, it can be seen that the encapsulation efficiency of the four groups of micelle solutions is above 50%, but the drug loading difference is relatively large, the smallest drug loading is 0.723% and the highest drug loading is 4.706%.

Table S4. Orthogonal experimental design and statistical analysis.

Groups	A	B	C	Average loading efficiency (%)	Average encapsulation efficiency (%)
1	1	1	1	1.540	50.012
2	2	2	2	2.950	56.108
3	3	3	3	2.074	32.389
4	1	2	3	0.723	36.573
5	2	3	1	2.543	31.531
6	3	1	2	3.876	54.190
7	1	3	2	1.173	45.116
8	2	1	3	1.529	36.388
9	3	2	1	4.706	51.064
K ₁	43.900	46.863	44.202		
K ₂	41.342	47.915	51.805		
K ₃	45.881	36.345	35.117		
R	4.539	11.570	16.688		

According to the range analysis, the ratio of the aqueous phase to the oil phase has the greatest effect on the encapsulation efficiency and drug loading of PLGA-lysoGM1/DOX micelles, and then the carrier volume and finally the dose.

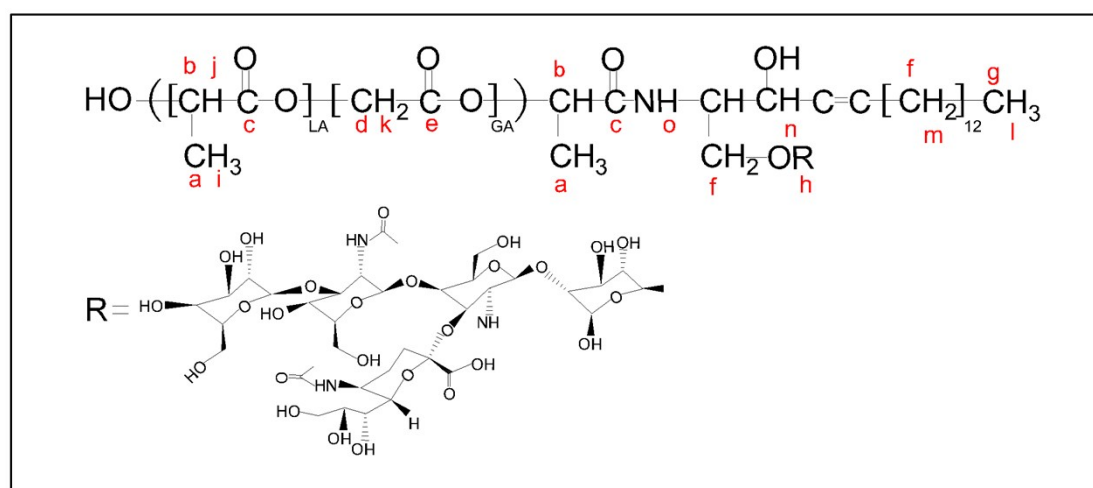


Figure S2. The structural formula of PLGA-lysoGM1. The carbon-based peaks and proton peaks are assigned as indicated in the Figure.

Table S5. Absorption bands concerning the PLGA-lysoGM1 and its attributions.

Absorption bands (cm⁻¹)	Attributions
3000 – 2700	CH, CH ₃ e CH ₂ (asymmetric stretching)
1760 – 1750	C=O (stretch)
1680 – 1630	Amide I band C=O (stretch)
1500 – 1250	CH ₃ e CH ₂ (symmetric angular deformation)
1350 – 1150	CH ₃ e CH ₂ (Symmetric deformation vibration)
1300 – 1150	C-O (stretch)

The absorption peaks of the infrared spectrum of PLGA-lysoGM1 are shown in Table S5. The absorption peak at 2995 cm⁻¹ and 2945 cm⁻¹ is the asymmetric stretching vibration of methyl and methylene groups. The strong absorption peak at 1755 cm⁻¹ belongs to the ester group in PLGA, and the other peaks are shown in the table.

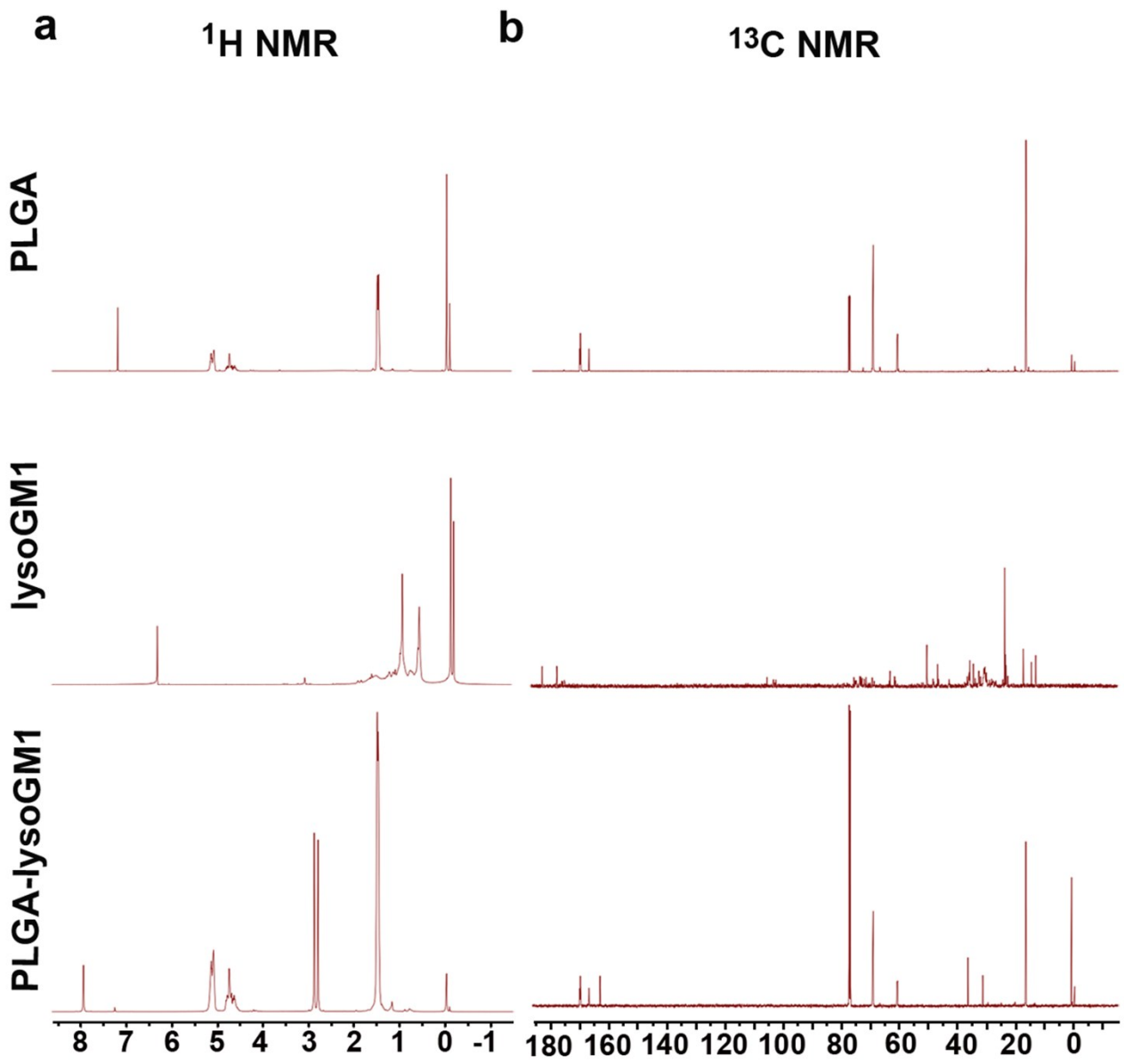


Figure S3. The ^1H NMR spectrum and ^{13}C NMR spectrum.



Figure S4. (a) The surface potential of PLGA-lysoGM1 micelles was -34.9 mV. (b) The surface potential of PLGA-lysoGM1/DOX micelles was -33.2 mV.

The calibration curve of DOX in PBS buffer was established at 480 nm, and a linear relationship was obtained with a correlation coefficient of 0.9996 (pH 5.4) and 0.9998 (pH 7.4).

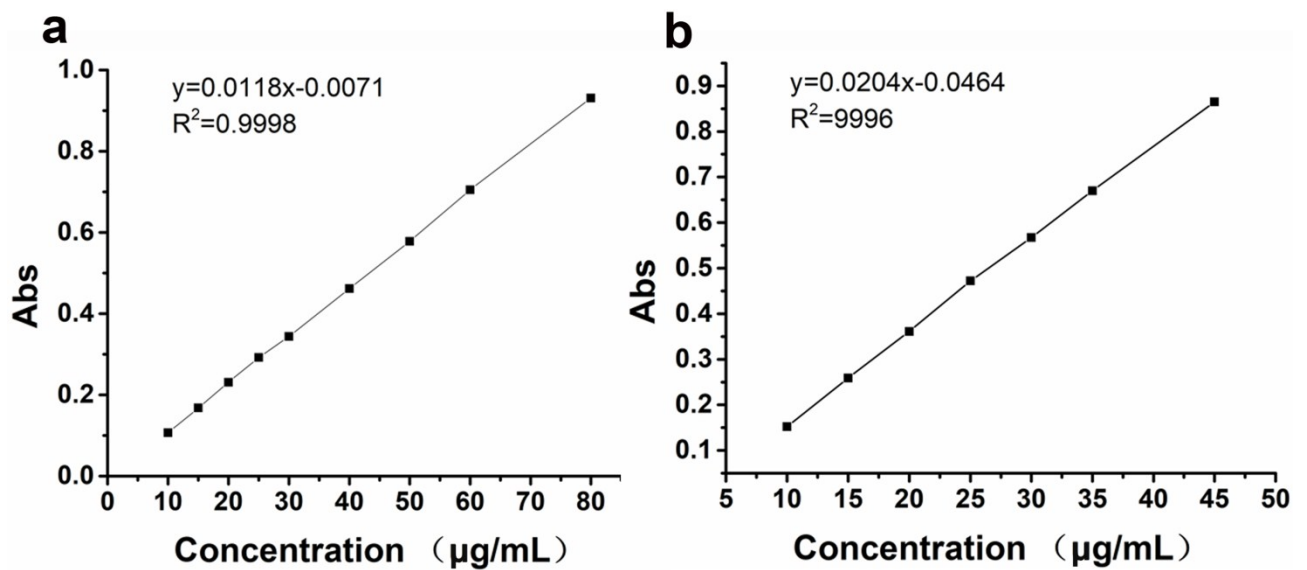


Figure S5. The standard curve of DOX in PBS solution. (a) The regression equation is $y=0.0118x-0.0071$, $R^2=0.9998$, pH5.4. (b) The regression equation is $y=0.0204x-0.0464$, $R^2=0.9996$, pH7.4.

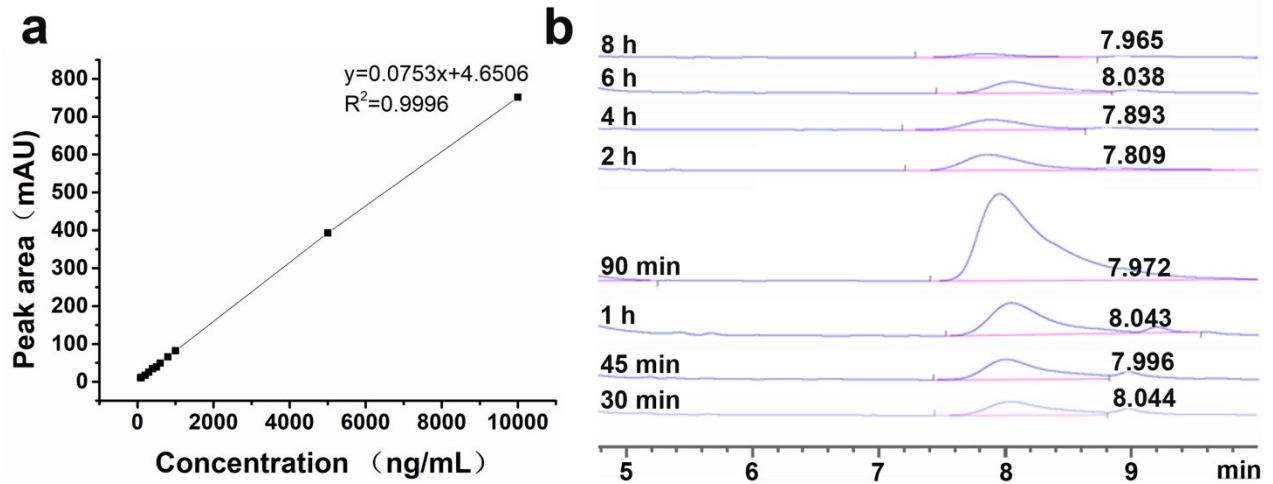


Figure S6. (a) The standard curve of DOX in HPLC. The regression equation is $y=0.0753x+4.6506$, $R^2=0.9996$.

(b) Detecting the distribution of DOX in CSF by HPLC at different time. The peak time is about 8 min. The peak area increases first and then decreases.

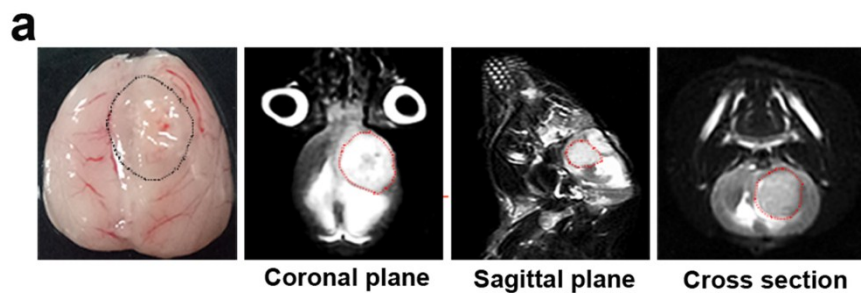


Figure S7. These MRI images of C6 glioma-bearing rats.

Supplementary References

1. Y. Liu, K. Tang, W. Yan, Y. Wang, G. You, C. Kang, T. Jiang and W. Zhang, *Neurosci Lett*, 2013, **546**, 36-41.